CrystEngComm

Accepted Manuscript

This is an *Accepted Manuscript*, which has been through the Royal Society of Chemistry peer review process and has been accepted for publication.

Accepted Manuscripts are published online shortly after acceptance, before technical editing, formatting and proof reading. Using this free service, authors can make their results available to the community, in citable form, before we publish the edited article. We will replace this *Accepted Manuscript* with the edited and formatted *Advance Article* as soon as it is available.

You can find more information about *Accepted Manuscripts* in the Information for Authors.

Please note that technical editing may introduce minor changes to the text and/or graphics, which may alter content. The journal's standard Terms & Conditions and the Ethical guidelines still apply. In no event shall the Royal Society of Chemistry be held responsible for any errors or omissions in this *Accepted Manuscript* or any consequences arising from the use of any information it contains.

ROYAL SOCIETY OF CHEMISTRY

www.rsc.org/crystengcomm

Cite this: DOI: 10.1039/c0xx00000x

www.rsc.org/xxxxxx

COMMUNICATION

Structural modification in bimetallic Ru(III)-Co(II) metal-organic frameworks

Shenshen Li,[a] Yu-Sheng Chen,[b] and Karen L. Mulfort*[a]

Received (in XXX, XXX) Xth XXXXXXXXX 20XX, Accepted Xth XXXXXXXXX 20XX

DOI: 10.1039/b000000x

Two new mixed-metal MOFs were synthesized using the same $Ru_3O(OAc)_6^+$-based struts and Co(II)-based nodes but variation in synthesis conditions have yielded markedly different topology.

A handful of seminal studies have recently described the interaction of visible light energy with a variety of metal-organic framework (MOF) structures, specifically targeted toward efficient and robust light-harvesting and photocatalysis. These reports have revealed long-range,[1] ultrafast,[2] and through-pore energy[3, 4] and electron transfer,[5] interfacial energy[6] and electron transfer,[7] photocatalysis,[8] and generally demonstrate the enormous potential of MOF architectures to significantly impact the drive toward efficient materials for applications such as photovoltaics and artificial photosynthesis. Since this is a relatively new field for MOFs, the impact of structure on the behaviour of photons and photon-to-energy conversion within the porous networks has not yet been fully examined. Directed synthesis efforts are necessary to yield new structures which will contribute to a fundamental understanding of how light interacts with MOFs and to guide ongoing design principles. In this vein, we have initiated a research program to examine the impact of variations in MOF structure on the primary photochemistry and pathways for redox and light-driven electron transfer between donors and acceptors. Notably, MOFs present opportunities to incorporate identical chemical modules as struts and nodes, and to build a variety of architectures that probe structural factors unique to the MOF platform (i.e. topology, strut/node connectivity, pore size, pore guests) that cannot be replicated in homogeneous molecular or supramolecular systems.

Herein we describe the synthesis and single crystal structural determination of two new mixed-metal MOF structures with strong potential for redox- and photo-activity. We have specifically targeted the $Ru_3O(OAc)_6^+$ cluster as a strut in new MOF architectures since it is known for its broad spectral coverage, rich redox chemistry, multi-electron transfer processes, and facile cluster-to-cluster electron transfer.[9-12] When labile solvent coordination at Ru(III) is replaced by isonicotinic acid (pyCOOH), the resulting $Ru_3O(OAc)_6(pyCOOH)_3^+$ cluster represents a bulky, visible-light absorbing, redox-active analogue to commonly used tri-carboxylate struts[13-15] (Figure 1). Similar M_3-μ_3-O clusters (where M = Al,[16] Cr,[17] Fe,[18] Sc,[19] V[20] for example) have been employed in the development of many MOFs, however, to the best of our knowledge, this is the first appearance of the $Ru_3O(OAc)_6^+$ cluster in an extended coordination polymer. We selected cobalt as the node metal as it has multiple accessible coordination environments and often leaves unsaturated coordination sites on which to bind variable small molecule substrates.[13, 21, 22] Furthermore, cobalt is a key element in schemes for artificial photosynthesis in both water oxidation[23] and proton reduction[24] and we have interest in using the resultant MOFs as photocatalysts for solar energy conversion. And generally, heterometallic MOFs are relatively rare[25-28] and may present additional opportunities for bifunctional or cooperative catalysis.[29]

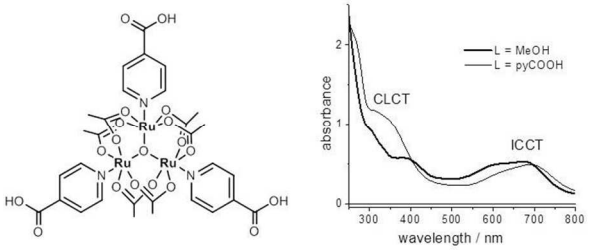

Figure 1. Left: chemical structure of $Ru_3O(OAc)_6(pyCOOH)_3^+$ strut used in synthesis of mixed-metal MOFs. Right: ground state absorbance of $Ru_3O(OAc)_6(L)_3^+$ in methanol where L represents the axial Ru(III) ligand. Cluster-to-ligand charge transfer (CLCT) and intra-cluster charge transfer (ICCT) bands result in broad absorbance across UV and visible regions.

New MOF synthesis was accomplished by heating a solution of $[Ru_3O(OAc)_6(pyCOOH)_3]PF_6$ and $Co(NO_3)_2{\cdot}6H_2O$ in dimethylacetamide at 50°C for 200 hours and yielded intensely dark green ellipsoidal crystals approximately 30 μm in length (full details in the ESI). We detected only very weak diffraction with traditional lab X-ray sources so we turned to the microcrystallography capabilities at ChemMatCARS at the Advanced Photon Source.[30] Single-crystal synchrotron X-ray diffraction analysis revealed the desolventized structure and composition of these crystals to be $[Ru_3O(OAc)_6(pyCOO)_3]_2[Co_3(OH)_2]$, **RuCo-1** (Figure 2).† There was significant disordered electron density within the pores of **RuCo-1** which was removed using the SQUEEZE routine of PLATON,[31] and yields a solvent-accessible void volume of 2408 Å^3, roughly 41% of the total crystal volume. **RuCo-1** crystallizes in the C2/m space group in an augmented (6,3)-c net consisting of stacked two-dimensional sheets separated by approximately 10.8Å. The sheets are composed of Co_3 nodes

CrystEngComm Accepted Manuscript

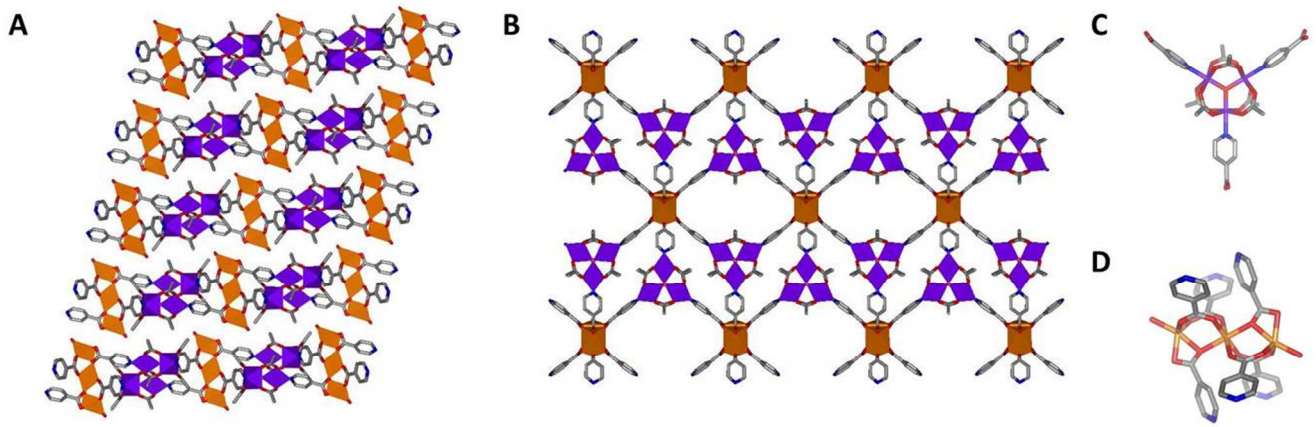

Figure 2. Crystal structure of **RuCo-1**. Gray, carbon; blue, nitrogen; red, oxygen; orange, cobalt; purple, ruthenium; hydrogen atoms omitted for clarity. A) Stacking of two-dimensional sheets. B) Top view of hexagonal coordination of Co_3 node with six different Ru_3O struts within a single sheet. C) Detail of $Ru_3O(OAc)_6(pyCOO)_3^{2-}$ strut. D) Detail of Co_3 node which coordinates six $pyCOO^-$ groups and two hydroxyl groups.

which are hexagonally-coordinated by Ru_3O-based struts (Figure 2B). Each Ru_3O is directly connected to three Co_3 nodes in the same sheet, while each Co_3 node is bound to six neighbouring Ru_3O struts. The $[Ru_3O(OAc)_6(pyCOO)_3]^{2-}$ strut in the MOF has similar bond lengths and angles as previously reported molecular crystal structures containing the $Ru_3O(OAc)_6^+$ cluster (Table 1, Table S2).[32-34] The Co_3 nodes are formed during the self-assembly process from the Co(II) ions and the carboxylate end of the isonicotinate linkers that extend out from the Ru_3O cores. The central cobalt of each node sits on an inversion centre, is coordinated by six carboxylate oxygen atoms from six different $[Ru_3O(OAc)_6(pyCOO)_3]^{2-}$ struts, and contains a near-octahedral ligand field. The two edge cobalt atoms of **RuCo-1** are coordinated by five oxygen atoms in a trigonal bipyramidal environment, the fifth coordination is a terminal oxygen atom with a Co-O distance of 2.046 Å, which we have assigned as Co-OH coordination considering bond length and overall charge balance. This linear M_3 structure is similar to those previously described in cobalt-based MOFs (i.e. Co-PIZA,[35] DUT-28[36]) and multimetallic sites bridged by carboxylates is a recurring motif in metalloprotein active site and models.[37] The possibility to remove or exchange the hydroxyl ligands under appropriate conditions presents the opportunity for small molecule activation and catalysis at the Co nodes.

In optimizing the synthesis of the $[Ru_3O(OAc)_6(pyCOOH)_3](PF_6)$ strut, we observed ligand scrambling at elevated temperature as pyCOOH vacates the Ru(III) axial position and its carboxylate group replaces the cluster acetate groups as Ru(III) bridging ligands. We therefore hypothesized that by performing MOF synthesis at elevated temperatures, we could encourage ligand scrambling to vary the strut/node connectivity. Additionally, this may open up the Ru(III) axial positions as potential binding sites to post-synthetically modulate the Ru_3O strut redox properties or as substrate binding sites for catalytic transformations. This ligand exchange strategy has been described previously in the design of breathing frameworks, and successfully used to replace acetate bridges on Fe_3O clusters with ditopic muconates.[18]

Consequently, conditions similar to those used for the synthesis of **RuCo-1** at a slightly higher temperature (80°C, full details in ESI) yielded dark green crystals with a flattened octahedral shape. Single crystal synchrotron X-ray diffraction revealed an entirely different composition and structure, $[Ru_3O(OAc)_6(pyCOO)_3]_6[Ru_3O(H_2O)_3]_2Co_3(OH)_2X_6$, **RuCo-2** (Figure 3), where X represents framework charge balancing anions disordered in the pores.† The SQUEEZE routine of PLATON was used to remove disordered electron density within the pores of **RuCo-2**, and yields approximately 66% of the crystal as solvent-accessible void volume. **RuCo-2** crystallizes in the C2/m space group in an augmented (12,6)-c net and is composed of nearly identical struts and nodes as **RuCo-1**. Like **RuCo-1**, this crystal can be seen as a series of sheets, shown in

Table 1. Selected bond lengths (Å) for **RuCo-1**, **RuCo-2**, and related molecular Ru_3O complexes.

structure	Ru-$O_{central}$	Ru-Ru	Ru-L	Ru-$O_{acetate}$	ref
RuCo-1	1.903	3.3145	2.089(5)		this work
	1.921	3.3145	2.089(5)	1.99-2.01	
	1.921	3.3227(6)	2.121		
RuCo-2					this work
Ru_3O^A	1.84(1)	3.302(3)	2.11(1)		
	1.92(1)	3.304(3)	2.13(2)	1.95-2.13	
	1.99(1)	3.338(3)	2.16(2)		
Ru_3O^B	2.03	3.51	2.10(1)		
	2.032	3.51	2.10(1)	2.04-2.11	
	2.032	3.539(4)	2.19		
$Ru_3O(OAc)_6(py)_3PF_6$	1.913(3)	3.3380(6)	2.092(4)		33
	1.943(4)	3.3480(6)	2.104(4)	2.02-2.05	
	1.947(4)	3.3636(7)	2.109(5)		
$Ru_3O(OAc)_6(H_2O)_3ClO_4$	1.889(3)	3.2884(8)	2.102(5)		32
	1.897(3)	3.2888(8)	2.121(5)	2.01-2.04	
	1.927(4)	3.3165(9)	2.141(5)		
$Ru_3O(OBz)_6(py)_3PF_6$	1.934	3.349(2)	2.13(1)		31
	1.935	3.349(2)	2.134(6)	2.01-2.03	
	1.935	3.349(3)	2.134(9)		

CrystEngComm Accepted Manuscript

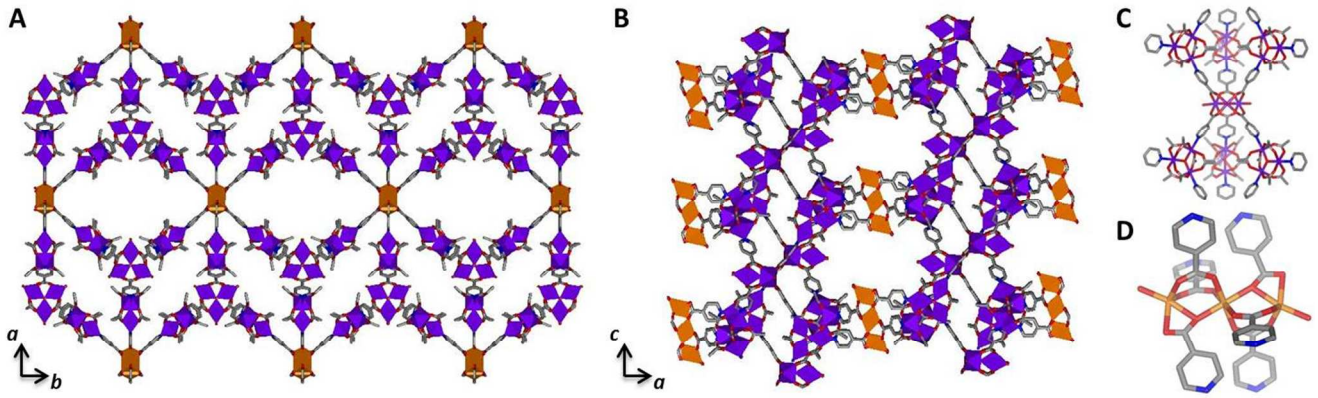

Figure 3. Crystal structure of **RuCo-2**. Gray, carbon; blue, nitrogen; red, oxygen; orange, cobalt; purple, ruthenium; hydrogen atoms omitted for clarity. A) View down *c*-axis showing three-dimensional structure. B) View down *b*-axis showing three-dimensional structure. C) Detail of Ru_3O^A and Ru_3O^B struts and interconnectivity. D) Detail of Co_3 node which coordinates six $pyCOO^-$ groups and two hydroxyl groups.

Figure 3A) and stacked together along the *c* axis, although these sheets are tied together to form a 3-D structure, unlike **RuCo-1**. Interestingly, in one-fourth of the Ru_3O units, the acetate groups have been replaced by the carboxylate groups of pyCOOH, purportedly facilitated by the slightly more aggressive reaction conditions. Therefore, **RuCo-2** contains two types of Ru_3O-based struts. The first Ru_3O strut, noted Ru_3O^A, maintains the core structure of the starting material and its bond length and angle parameters agree with **RuCo-1** very well. The second type of Ru_3O strut, noted Ru_3O^B, is formed *in situ* via $pyCOO^-$ displacement of the acetate groups during MOF synthesis and its structure, with $pyCOO^-$ bridging and axial water ligands coordinating Ru(III), is distinctly different from Ru_3O^A even though the same general coordination is maintained (Table 1). Notably, the Ru-Ru distances in Ru_3O^B are substantially longer than in Ru_3O^A (~3.3Å in Ru_3O^A vs. >3.5Å in Ru_3O^B, see Table 1). The trigonal plane of Ru_3O^B lies orthogonal to all the Ru_3O^A planes, and from the perspective of the two-dimensional sheets described above, each Ru_3O^B sits half-way between the two sheets, and connects six Ru_3O^A at the N-terminus of its bridging $pyCOO^-$. Three of the Ru_3O^A belong to sheet above Ru_3O^B and three belong to the sheet below, so that the hexagonal two-dimensional sheets are connected via a Ru_3O^B knot to form the three-dimensional network of **RuCo-2**. From the perspective of Ru_3O^A, two of its three axial pyCOO- ligands are tied to the Ru_3O^B units above and below it respectively, while the third bonds the Co_3 clusters in the same sheet. The Co_3 node of **RuCo-2** is structurally very similar to that of **RuCo-1** (Table S2). The three cobalt atoms are arranged linearly, with the central cobalt at the inversion centre of the cluster and coordinated by six carboxylate oxygen atoms from six different $pyCOO^-$ ligands. The edge cobalt atoms sit in a distorted trigonal bipyramidal environment with a Co-OH bond length of 2.021 Å. These five-coordinated Co sites, as in **RuCo-1**, are potential binding sites for small molecule activations.

Direct comparison of the network topology between these two chemically similar frameworks reveals distinct differences with potential impact on the redox and electronic properties. **RuCo-1** can be considered to be a series of hexagons, made of $[Co_3][Ru_3O]_6$ units sharing common edges (Figure S1), whereas **RuCo-2** is much more topologically complex. It is easiest to treat the framework of **RuCo-2** as an interconnected binodal network. We have designated the first node as a matrix of hexagonal units consisting of $[Co_3][Ru_3O^A]_6$, similar to those in **RuCo-1**, see Figure S2. Each of the Ru clusters contributes two axial positions, both pointing out of the hexagonal plane, leading to a total of 12 extension points. Under this topological arrangement, the hexagons can no longer share edges to form two-dimensional sheets like in **RuCo-1**. Instead, they share corners with a second type of topological nodes, *i.e.* a series of $[Ru_3O^B]$ trigonal prisms each with six pyridyl arms. This forms a distinctly different (12, 6)-c network.

The inclusion of the Ru_3O cluster in **RuCo-1** and **RuCo-2** presents a promising step toward determination of electron transfer properties in diverse MOF architectures based on chemically identical modules. Importantly, based on an extensive body of work exploring the mixed valency and intervalence charge transfer between linked $Ru_3O(OAc)_6^+$ clusters,[12, 38] we can make direct comparisons to molecular and supramolecular analogues. We anticipate that the close proximity between Ru_3O struts and Co_3 nodes will enable substantial electronic communication in **RuCo-1** and **RuCo-2** as previously observed with Ru_3O clusters bound to Co porphyrins[39] or CdSe quantum dots.[40]

In summary, we have successfully synthesized two new bimetallic, potentially bifunctional, MOF architectures. **RuCo-1** is a two-dimensional MOF that includes both light-harvesting Ru_3O-based struts and potentially catalytic Co_3 nodes. **RuCo-2** is a three-dimensional MOF that was obtained by exploiting the thermal lability of Ru_3O-acetate coordination and the *in situ* creation of a new strut. As of yet we have only been able to grow single crystals of **RuCo-1** and **RuCo-2**, the reaction mixtures were contaminated with insoluble amorphous materials and attempts to isolate a pure quantity MOF purification or separation techniques were unsuccessful.[41] However, ongoing efforts are directed at using high-throughput capabilities[36, 42, 43] to screen conditions which will yield a pure structure in bulk quantities so that we can pursue electrochemical and photophysical characterization of both structures. However, these two new structures demonstrate the capability of synthesis-driven structural tailoring which can be used to design new, potentially photocatalytically-active MOFs. With these two new structures in

CrystEngComm Accepted Manuscript

hand, we intend to probe the effect of network topography on photoinduced electron transfer between the struts and nodes and directly compare the heterogeneous frameworks to homogeneous supramolecular analogues.

Acknowledgments

This material is based upon work supported by the U.S. Department of Energy, Office of Science, Office of Basic Energy Sciences, under contract number DE-AC02-06CH11357. S.L. thanks the Division of Chemical Sciences and Engineering for postdoctoral support. ChemMatCARS Sector 15 is principally supported by the National Science Foundation/Department of Energy under grant number NSF/CHE-1346572. Use of the Advanced Photon Source is supported by the U. S. Department of Energy, Office of Science, Office of Basic Energy Sciences, under Contract No. DE-AC02-06CH11357.

Notes and references

[a] *Division of Chemical Sciences and Engineering, Argonne National Laboratory, 9700 South Cass Avenue, Argonne IL 60439, USA. Tel: 630 252 3545; E-mail: mulfort@anl.gov*

[b] *ChemMatCARS, Advanced Photon Source, Argonne IL 60439, USA.*

† Electronic Supplementary Information (ESI) available: synthetic details of $Ru_3O(OAc)_6(pyCOOH)_3(PF_6)$, synthesis and crystallographic data for **RuCo-1** and **RuCo-2**. CCDC 1029004-1029005. For ESI and crystallographic data in CIF format see DOI: 10.1039/b000000x/

1. C. A. Kent, B. P. Mehl, L. Ma, J. M. Papanikolas, T. J. Meyer and W. Lin, *J. Am. Chem. Soc.*, 2010, **132**, 12767-12769.
2. H.-J. Son, S. Jin, S. Patwardhan, S. J. Wezenberg, N. C. Jeong, M. So, C. E. Wilmer, A. A. Sarjeant, G. C. Schatz, R. Q. Snurr, O. K. Farha, G. P. Wiederrecht and J. T. Hupp, *J. Am. Chem. Soc.*, 2012, **135**, 862-869.
3. C. Y. Lee, O. K. Farha, B. J. Hong, A. A. Sarjeant, S. T. Nguyen and J. T. Hupp, *J. Am. Chem. Soc.*, 2011, **133**, 15858-15861.
4. W. A. Maza and A. J. Morris, *J. Phys. Chem. C*, 2014, **118**, 8803-8817.
5. R. W. Larsen and L. Wojtas, *J. Mater. Chem. A*, 2013, **1**, 14133-14139.
6. S. Jin, H.-J. Son, O. K. Farha, G. P. Wiederrecht and J. T. Hupp, *J. Am. Chem. Soc.*, 2013, **135**, 955-958.
7. C. A. Kent, D. Liu, L. Ma, J. M. Papanikolas, T. J. Meyer and W. Lin, *J. Am. Chem. Soc.*, 2011, **133**, 12940-12943.
8. T. Zhang and W. Lin, *Chem. Soc. Rev.*, 2014, **43**, 5982-5993.
9. A. Spencer and G. Wilkinson, *J. Chem. Soc. Dalton Trans.*, 1972, 1570-1577.
10. J. A. Baumann, D. J. Salmon, S. T. Wilson, T. J. Meyer and W. E. Hatfield, *Inorg. Chem.*, 1978, **17**, 3342-3350.
11. H. E. Toma, K. Araki, A. D. P. Alexiou, S. Nikolaou and S. Dovidauskas, *Coord. Chem. Rev.*, 2001, **219-221**, 187-234.
12. C. P. Kubiak, *Inorg. Chem.*, 2013, **52**, 5663-5676.
13. S. Ma and H.-C. Zhou, *J. Am. Chem. Soc.*, 2006, **128**, 11734-11735.
14. H. K. Chae, D. Y. Siberio-Perez, J. Kim, Y. Go, M. Eddaoudi, A. J. Matzger, M. O'Keeffe and O. M. Yaghi, *Nature*, 2004, **427**, 523-527.
15. S. S. Y. Chui, S. M. F. Lo, J. P. Charmant, A. G. Orpen and I. D. Williams, *Science*, 1999, **283**, 1148-1150.
16. C. Volkringer, D. Popov, T. Loiseau, G. Férey, M. Burghammer, C. Riekel, M. Haouas and F. Taulelle, *Chem. Mater.*, 2009, **21**, 5695-5697.
17. G. Férey, C. Mellot-Draznieks, C. Serre, F. Millange, J. Dutour, S. Surblé and I. Margiolaki, *Science*, 2005, **309**, 2040-2042.
18. C. Serre, F. Millange, S. Surblé and G. Férey, *Angew. Chem., Int. Ed.*, 2004, **43**, 6285-6289.
19. J. P. S. Mowat, S. R. Miller, A. M. Z. Slawin, V. R. Seymour, S. E. Ashbrook and P. A. Wright, *Microporous Mesoporous Mater.*, 2011, **142**, 322-333.
20. K. Barthelet, D. Riou and G. Ferey, *Chem. Commun.*, 2002, 1492-1493.
21. Y. Chen, J. Zhang, J. Li and J. V. Lockard, *J. Phys. Chem. C*, 2013, **117**, 20068-20077.
22. N. Nijem, L. Kong, Y. Zhao, H. Wu, J. Li, D. C. Langreth and Y. J. Chabal, *J. Am. Chem. Soc.*, 2011, **133**, 4782-4784.
23. D. G. Nocera, *Acc. Chem. Res.*, 2012, **45**, 767-776.
24. V. Artero, M. Chavarot-Kerlidou and M. Fontecave, *Angew. Chem., Int. Ed.*, 2011, **50**, 7238-7266.
25. A. Schoedel, L. Wojtas, S. P. Kelley, R. D. Rogers, M. Eddaoudi and M. J. Zaworotko, *Angew. Chem., Int. Ed.*, 2011, **50**, 11421-11424.
26. A. Hazra, P. Kanoo and T. K. Maji, *Chem. Commun.*, 2011, **47**, 538-540.
27. J. R. Stork, V. S. Thoi and S. M. Cohen, *Inorg. Chem.*, 2007, **46**, 11213-11223.
28. C. L. Cahill, D. T. de Lill and M. Frisch, *CrystEngComm*, 2007, **9**, 15-26.
29. A. Dhakshinamoorthy and H. Garcia, *ChemSusChem*, 2014, **7**, 2392-2410.
30. ChemMatCARS, https://chemmatcars.uchicago.edu/page/advanced-crystallography, Accessed September 4, 2014.
31. A. L. Spek, *J. Appl. Crystallogr.*, 2003, **36**, 7-13.
32. M. Abe, Y. Sasaki, T. Yamaguchi and T. Ito, *Bull. Chem. Soc. Jpn.*, 1992, **65**, 1585-1590.
33. J. C. Goeltz, E. E. Benson and C. P. Kubiak, *J. Phys. Chem. B*, 2010, **114**, 14729-14734.
34. G. Powell, D. T. Richens and A. Bino, *Inorg. Chim. Acta*, 1995, **232**, 167-170.
35. M. E. Kosal, J.-H. Chou, S. R. Wilson and K. S. Suslick, *Nat Mater*, 2002, **1**, 118-121.
36. P. Wollmann, M. Leistner, U. Stoeck, R. Grunker, K. Gedrich, N. Klein, O. Throl, W. Grahlert, I. Senkovska, F. Dreisbach and S. Kaskel, *Chem. Commun.*, 2011, **47**, 5151-5153.
37. E. Y. Tshuva and S. J. Lippard, *Chem. Rev.*, 2004, **104**, 987-1012.
38. S. D. Glover, J. C. Goeltz, B. J. Lear and C. P. Kubiak, *Coord. Chem. Rev.*, 2010, **254**, 331-345.
39. K. Araki, S. Dovidauskas, H. Winnischofer, A. D. P. Alexiou and H. E. Toma, *J. Electroanal. Chem.*, 2001, **498**, 152-160.
40. A. J. Morris-Cohen, K. O. Aruda, A. M. Rasmussen, G. Canzi, T. Seideman, C. P. Kubiak and E. A. Weiss, *Phys. Chem. Chem. Phys* . 2012, **14**, 13794-13801.
41. O. K. Farha and J. T. Hupp, *Acc. Chem. Res.*, 2010, **43**, 1166-1175.
42. S. Bauer, C. Serre, T. Devic, P. Horcajada, J. r. m. Marrot, G. r. Férey and N. Stock, *Inorg. Chem.*, 2008, **47**, 7568-7576.
43. R. Banerjee, A. Phan, B. Wang, C. Knobler, H. Furukawa, M. O'Keeffe and O. M. Yaghi, *Science*, 2008, **319**, 939-943.

CrystEngComm Accepted Manuscript